

# Multidimensional Eigenwave Multiplexing Modulation for Non-Stationary Channels

Zhibin Zou, and Aveek Dutta

Department of Electrical and Computer Engineering  
University at Albany SUNY, Albany, NY 12222 USA  
{zzou2, adutta}@albany.edu

**Abstract**—While interference in time domain (caused by path difference) is mitigated by OFDM modulation, interference in frequency domain (due to velocity difference), can be mitigated by OTFS modulation. However, in non-stationary channels, the relative difference in acceleration will cause Inter-Doppler Interference (IDI) and a modulation method for mitigating IDI does not exist in the literature. Both methods in the literature use carriers in a specific domain which achieve orthogonality in the target domain to mitigate interference. Moreover, those modulation cannot directly incorporate space domain, which requires additional precoding technique to mitigate inter-user interference (IUI) for MU-MIMO channels. This work presents a generalized modulation for any multidimensional channel. Recently, Higher Order Mercer’s Theorem (HOGMT) [1] has been proposed to decompose multi-user non-stationary channels into independent fading subchannels (Eigenwaves). Based on HOGMT decomposition, we develop Multidimensional Eigenwaves Multiplexing (MEM) modulation which uses jointly orthogonal eigenwaves, decomposed from the multidimensional channel as subcarriers. Data symbols modulated by these eigenwaves can achieve orthogonality across each degree of freedom (e.g., space (users/antennas), time-frequency and delay-Doppler). Consequently, the transmitted remain independent over the high dimensional channel, thereby avoiding interference from other symbols.

## I. INTRODUCTION

Path delays cause the Inter-Symbol Interference (ISI), which can be mitigated by OFDM as it transmits symbols in frequency domain [2]. On the other hand, Doppler effect causes Inter-Carrier Interference (ICI), which can be mitigated by OTFS modulation by transmitting symbols in the delay-Doppler domain [3], [4]. However, in non-stationary channels, both the delay and the Doppler effects changes over time and frequency, which leads to interference at the delay-Doppler domain, which is also referred as Inter-Doppler Interference (IDI) [5]. Detectors have been investigated to mitigate IDI for OTFS symbols [5], [6]. However, these additional techniques can not ensure interference-free at the delay-Doppler domain, especially for highly non-stationary channels. Those techniques are iteratively developed to mitigate ISI, ICI and then IDI due to path difference  $\Delta x$ , velocity difference  $\Delta x'$  and then acceleration difference  $\Delta x''$ , by investigating orthogonality at time, time-frequency, and delay-Doppler domain, respectively. In general, modulation techniques design carriers in the domain represented by high order physics as it is relatively less variant with minimal interference. This motivates us to investigate a general modulation for high dimensional channels. Moreover, the above modulations can not directly

Table I: Comparison between OTFS and MEM

Modulations	OTFS	MEM
Mathematical tool	SFT	HOGMT
Carriers domain	Delay-Doppler domain	Eigen domain
CSI requirement	CSI at Rx	CSI at TX and Rx
Adaptive to NS channels	No	Yes
General to HD channels	No	Yes

incorporate space domain, therefore requiring additional precoding techniques to cancel spatial interference for MU-MIMO channels [7], [8]. In this paper, we present a general high dimensional modulation for non-stationary channels<sup>1</sup>. Recently, HOGMT has been proposed as a mathematical tool for multi-user non-stationary channel decomposition [1]. It can decompose the high-dimensional channels into independent subchannels along each degree of freedom (DoF). We leverage this tool to develop Multidimensional Eigenwave Multiplexing (MEM) modulation which uses the jointly orthogonal eigenwaves decomposed from the high dimensional channel as carriers. Symbols on these carriers achieve orthogonality across each DoF and thus avoid interference from all DoF.

We summarize the qualitative differences between OTFS and MEM in Table I. OTFS obtains the carriers by Symplectic Fourier Transform (SFT), while MEM obtains its carriers by HOGMT. The OTFS carriers are in the delay-Doppler domain, while carriers of MEM are at the eigen domain. Further, OTFS requires CSI at the receiver side only, while MEM requires CSI at both transmitter and receiver side. This is the main cost of MEM, although the CSI is generally required at the transmitter in modern wireless systems that is well documented in the literature [9]. The OTFS input-output relation and the corresponding modulation schemes for non-stationary channels does not exist currently and it cannot directly generalize to higher dimensional channels. For instance, it requires additional precoding for MU-MIMO channels as it does not achieve spatial orthogonality. The details about the limitations of OTFS are discussed in Section III. The proposed MEM is able to achieve orthogonality for non-stationary channels and generalize to higher dimension, meaning it doesn’t require additional detector and precoding to cancel IDI and IUI.

The contribution of this paper is summarized as follows:

- We deduce the input-output relation for non-stationary

<sup>1</sup>Any channel can be generated as a special case of the non-stationary channel. Therefore the proposed modulation for non-stationary channels will certainly generalize to any and all wireless channels.

channels, which shows the variation across time-frequency and delay-Doppler domain.

- We design a multidimensional modulation with jointly orthogonal eigenwaves as subcarriers, cancelling interference in all degrees of freedom in non-stationary channels.
- We show the generality of MEM to higher dimensional channels and validate it by extending the channel to space domain (e.g., MU-MIMO channels) where MEM can also cancel spatial interference without additional precoding.
- We validate MEM under three channels, two of which shows the performance in non-stationary channels with different non-stationarity intervals. The third shows it's generality by incorporating the spatial domain.

## II. BACKGROUND

### A. Non-stationary wireless channel model

The wireless channel is typically expressed by a linear operator  $H$ , and the received signal  $r(t)$  is given by  $r(t)=Hs(t)$ , where  $s(t)$  is the transmitted signal. The physics of the impact of  $H$  on  $s(t)$  is described using the delays and Doppler shift in the multipath propagation [10] given by (1),

$$r(t) = \sum_{p=1}^P h_p s(t - \tau_p) e^{j2\pi\nu_p t} \quad (1)$$

where  $h_p$ ,  $\tau_p$  and  $\nu_p$  are the path attenuation factor, time delay and Doppler shift for path  $p$ , respectively. (1) is expressed in terms of the overall delay  $\tau$  and Doppler shift  $\nu$  [10] in (2),

$$r(t) = \iint S_H(\tau, \nu) s(t-\tau) e^{j2\pi\nu t} d\tau d\nu \quad (2)$$

$$= \int L_H(t, f) S(f) e^{j2\pi t f} df = \int h(t, \tau) s(t-\tau) d\tau \quad (3)$$

where  $S_H(\tau, \nu)$  is the (delay-Doppler) spreading function of channel  $H$ , which describes the combined attenuation factor for all paths in the delay-Doppler domain.  $S(f)$  is the Fourier transform of  $s(t)$  and the time-frequency (TF) domain representation of  $H$  is characterized by its TF transfer function,  $L_H(t, f)$  which can be obtained by 2-D Fourier transform as (4). The time-varying impulse response  $h(t, \tau)$  is obtained as the Inverse Fourier transform of  $S_H(\tau, \nu)$  from the Doppler domain to the time domain as in (5).

$$L_H(t, f) = \iint S_H(\tau, \nu) e^{j2\pi(t\nu - f\tau)} d\tau d\nu \quad (4)$$

$$h(t, \tau) = \int S_H(\tau, \nu) e^{j2\pi t \nu} d\nu \quad (5)$$

Figure 1 shows a general Linear Time Varying (LTV) channel model, represented in different domains and illustrates the mutual relationship between  $h(t, \tau)$ ,  $L_H(t, f)$  and  $S_H(\tau, \nu)$ .

### B. Statistics of non-stationary channels

For stationary channels, the TF transfer function is a stationary process and the spreading function is a white process (uncorrelated scattering) which are related as,

$$\mathbb{E}\{L_H(t, f)L_H^*(t', f')\} = R_H(t-t', f-f') \quad (6)$$

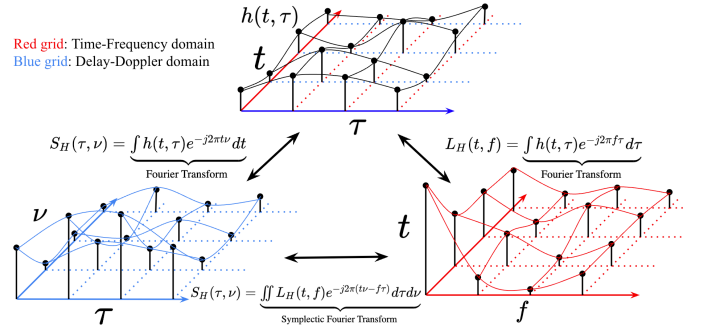


Figure 1: General LTV model transition in 4-D domain (time, frequency, delay and Doppler) [10], [11], [12].

$$\mathbb{E}\{S_H(\tau, \nu)S_H^*(\tau', \nu')\} = C_H(\tau, \nu)\delta(\tau-\tau')\delta(\nu-\nu') \quad (7)$$

where  $\delta(\cdot)$  is the Dirac delta function.  $C_H(\tau, \nu)$  and  $R_H(t-t', f-f')$  are the scattering function and TF correlation function, respectively, which are related via 2-D Fourier transform,

$$C_H(\tau, \nu) = \iint R_H(\Delta t, \Delta f) e^{-j2\pi(\nu\Delta t - \tau\Delta f)} d\Delta t d\Delta f \quad (8)$$

In contrast, for non-stationary channels, the TF transfer function is a non-stationary process and the spreading function is a non-white process. Therefore, a local scattering function (LSF)  $\mathcal{C}_H(t, f; \tau, \nu)$  [11] is defined to extend  $C_H(\tau, \nu)$  to non-stationary channels in (9). Similarly, the channel correlation function (CCF)  $\mathcal{R}(\Delta t, \Delta f; \Delta \tau, \Delta \nu)$  generalizes  $R_H(\Delta t, \Delta f)$  to the non-stationary case in (10).

$$\begin{aligned} \mathcal{C}_H(t, f; \tau, \nu) &= \iint R_L(t, f; \Delta t, \Delta f) e^{-j2\pi(\nu\Delta t - \tau\Delta f)} d\Delta t d\Delta f \quad (9) \\ &= \iint R_S(\tau, \nu; \Delta \tau, \Delta \nu) e^{-j2\pi(t\Delta \nu - f\Delta \tau)} d\Delta \tau d\Delta \nu \\ &\mathcal{R}(\Delta t, \Delta f; \Delta \tau, \Delta \nu) \\ &= \iint R_L(t, f; \Delta t, \Delta f) e^{-j2\pi(\Delta \nu t - \Delta \tau f)} dt df \quad (10) \\ &= \iint R_S(\tau, \nu; \Delta \tau, \Delta \nu) e^{-j2\pi(\Delta t \nu - \Delta f \tau)} d\tau d\nu \end{aligned}$$

where,  $R_L(t, f; \Delta t, \Delta f) = \mathbb{E}\{L_H(t, f+\Delta f)L_H^*(t-\Delta t, f)\}$  and  $R_S(\tau, \nu; \Delta \tau, \Delta \nu) = \mathbb{E}\{S_H(\tau, \nu+\Delta \nu)S_H^*(\tau-\Delta \tau, \nu)\}$ . For stationary channels, CCF reduces to TF correlation function  $\mathcal{R}(\Delta t, \Delta f; \Delta \tau, \Delta \nu) = R_H(\Delta t, \Delta f)\delta(\Delta t)\delta(\Delta f)$ .

## III. LIMITATIONS OF OTFS

**OTFS input-output relation:** The OTFS delay-Doppler input-output relation [4] can be rewritten in continuous form as,

$$r(t, f) = \iint h_w(\tau, \nu) s(t-\tau, f-\nu) d\tau d\nu + v(t, f) \quad (11)$$

where  $v(\tau, \nu)$  is noise, and  $h_w(\tau, \nu)$  is the twisted convolution of delay-Doppler response,  $h_c(\tau, \nu)$  with window function  $w(\tau, \nu)$  (Heisenberg transform) as in (12),

$$h_w(\tau, \nu) = \iint e^{-j2\pi\nu\nu'\tau'} h_c(\tau', \nu') w(\nu-\nu', \tau-\tau') d\tau' d\nu' \quad (12)$$

and relation of spreading function  $S_H(\tau, \nu)$  and delay-Doppler response  $h_c(\tau, \nu)$ , as given in [12] is,

$$S_H(\tau, \nu) = e^{-j2\pi\nu'} h_c(\tau, \nu) \quad (13)$$

Then (12) is rewritten as

$$h_w(\tau, \nu) = \iint S_H(\tau', \nu') w(\nu - \nu', \tau - \tau') d\tau' d\nu' \quad (14)$$

Notice  $h_w(\tau, \nu)$  is the flipped correlation of spreading function and a window function, i.e.,  $h_w(\tau, \nu) = \mathbb{E}\{S_H(\tau', \nu') w(\nu - \nu', \tau - \tau')\}$ , which is the correlation for stationary channels. *Currently, the model of OTFS input-output relation for non-stationary channels is not available in the literature.*

**Limitations of OTFS in non-stationary channels:** For non-stationary channels, we have  $\mathbb{E}\{S_H(\tau', \nu') w(\nu - \nu', \tau - \tau')\} = h_w(\tau', \nu'; \tau, \nu)$ . Then  $h_w(\tau, \nu)$  can be extended to time- and frequency-varying case to  $h_w(t, f; \tau, \nu)$  as,

$$\begin{aligned} h_w(t, f; \tau, \nu) &\triangleq \mathbb{F}^2\{\mathbb{E}\{S_H(\tau', \nu') w(\nu - \nu', \tau - \tau')\}\} \\ &= \iint h_w(\tau', \nu'; \tau, \nu) \times e^{j2\pi(t\nu' - f\tau')} d\tau' d\nu' \end{aligned} \quad (15)$$

where  $\mathbb{F}^2$  is the Symplectic Fourier Transform (SFT), i.e., 2-D Fourier Transform. Therefore OTFS input-output relation (11) for non-stationary channel is reformulated as,

$$r(t, f) = \iint h_w(t, f; \tau, \nu) s(t - \tau, f - \nu) d\tau d\nu + v(t, f) \quad (16)$$

Note that (16) has a similar form as (11) but shows the time and frequency variation of the impulse response function  $h_w(\tau, \nu)$ . Therefore we call  $h_w(t, f; \tau, \nu)$  as *local delay-Doppler response* (LDR) as defined by (15). The above deduction shows that OTFS modulation cannot be applied directly to non-stationary channels as it cannot deal with the LDR, which leads to interference in the delay-Doppler domain. *Currently, the OTFS modulation for non-stationary channels is not available in the literature.*

**Limitations of OTFS in higher dimensional channels:** Consider the deduced OTFS input-output relation for non-stationary channels in (16). Let  $k(t, f; t', f') \triangleq h_w(t, f; t - t', f - f')$  be the channel kernel, then (16) is rewritten as,

$$r(t, f) = \iint k(t, f; t', f') s(t', f') dt' df' + v(t, f) \quad (17)$$

For MU-MIMO non-stationary channels,  $h_w(t, f; \tau, \nu)$  is extended to  $\mathbf{H}(t, f; \tau, \nu)$ . For notational convenience, we use  $u$  and  $u'$  to represent a continuous space domain (users/antennas) at the receiver and transmitter, respectively. Then  $\mathbf{H}(t, f; \tau, \nu)$  is henceforth rewritten as  $h_w(u, t, f; u', \tau, \nu)$  and thus (17) can also be extended to MU-MIMO case as in (18),

$$\begin{aligned} r(u, t, f) &= \iiint k(u, t, f; u', t', f') s(u', t', f') du' dt' df' \\ &\quad + v(u, t, f) \end{aligned} \quad (18)$$

where  $k(u, t, f; u', t', f') \triangleq h_w(u, t, f; u', t - t', f - f')$  denotes the space-time-frequency transfer function. The OTFS symbol is not able to achieve joint orthogonality at space-time-

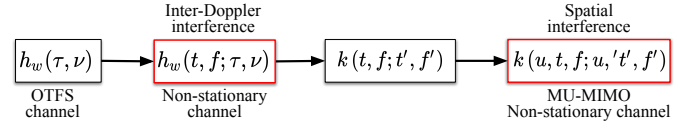


Figure 2: OTFS channel model evolution

frequency domain thereby leading to not only the spatial interference but also the joint space-time-frequency interference.

In conclusion, OTFS modulation has the limitations: 1) OTFS cannot deal with non-stationary channels where the delay-Doppler response is time- and frequency-varying. 2) OTFS require additional equalizer for MU-MIMO channels. Moreover, the equalizer and OTFS can only achieve the optimal interference cancellation at space and time-frequency domain respectively, as modulation and equalizers are independent processes. It is not able to achieve the global optimization for the joint space-time-frequency interference cancellation. Figure 2 shows the limitation of OTFS as the channel exhibits non-stationarity and is extended to higher dimension (space domain), where the models of OTFS are not available.

## IV. EIGENWAVE MODULATION

### A. HOGMT decomposition - a brief background

In [1], authors derived a generalized version of Mercer's Theorem [13] for asymmetric kernels and extended it to higher-order kernels, which decomposes an asymmetric multidimensional channel into jointly orthogonal subchannels. For any multidimensional process  $K(\zeta_1, \dots, \zeta_P; \gamma_1, \dots, \gamma_Q)$ , it can be decomposed by Theorem 1 in [1] as,

$$K(\zeta_1, \dots, \zeta_P; \gamma_1, \dots, \gamma_Q) = \sum_{n=1}^N \sigma_n \psi_n(\zeta_1, \dots, \zeta_P) \phi_n(\gamma_1, \dots, \gamma_Q)$$

where  $\mathbb{E}\{\sigma_n \sigma_n'\} = \lambda_n \delta_{nn'}$ .  $\lambda_n$  is the  $n^{\text{th}}$  eigenvalue.  $\{\phi_n\}$  and  $\{\psi_n\}$  are eigenfunctions having orthonormal property as,

$$\begin{aligned} \int \dots \int \phi_n(\gamma_1, \dots, \gamma_Q) \phi_{n'}(\gamma_1, \dots, \gamma_Q) d\gamma_1, \dots, d\gamma_Q &= \delta_{nn'} \\ \int \dots \int \psi_n(\zeta_1, \dots, \zeta_P) \psi_{n'}(\zeta_1, \dots, \zeta_P) d\zeta_1, \dots, d\zeta_P &= \delta_{nn'} \end{aligned}$$

### B. Multidimensional Eigenwave Multiplexing modulation

We leverage the decomposition framework in [1] and redefine the eigenfunctions with multiple variables, which can be defined as eigenwaves in multiple dimensions.

**Lemma 1.** (Associative property of eigenwave set projection) Define  $\Phi_a = \sum_{n=1}^N a_n \phi_n(\gamma_1, \dots, \gamma_Q)$ , we have

$$\langle \Phi_a, \Phi_b^* \rangle = \langle \Phi_{ab}, \Phi^* \rangle = \langle \Phi, \Phi_{ab}^* \rangle \quad (19)$$

where  $\langle \cdot, \cdot \rangle$  is the eigenwave set projection operator.  $\phi_n(\gamma_1, \dots, \gamma_Q)$  is  $Q$  dimensional eigenfunction.

*Proof.* The proof is provided in Appendix A [14].  $\square$

**Theorem 1.** (Multidimensional Eigenwave Multiplexing Modulation and Matched Filter)

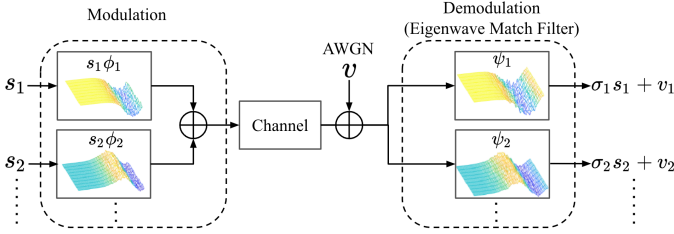


Figure 3: 2-D Eigenwave Multiplexing Modulation

Given, a  $M=Q+P$  dimensional channel transfer function  $H(\zeta_1, \dots, \zeta_P; \gamma_1, \dots, \gamma_Q)$  with input-output relation as

$$r(\zeta_1, \dots, \zeta_P) = \int \dots \int H(\zeta_1, \dots, \zeta_P; \gamma_1, \dots, \gamma_Q) s(\gamma_1, \dots, \gamma_Q) d\gamma_1, \dots, d\gamma_Q + v(\zeta_1, \dots, \zeta_P)$$

is decomposed into multidimensional eigenfunctions [1] as,

$$H(\zeta_1, \dots, \zeta_P; \gamma_1, \dots, \gamma_Q) = \sum_{n=1}^N \sigma_n \psi_n(\zeta_1, \dots, \zeta_P) \phi_n(\gamma_1, \dots, \gamma_Q)$$

then, a given symbol set,  $\{s_n\}$  is modulated using eigenfunctions  $\{\phi_n^*\}$  as subcarriers given by,

$$s(\zeta_1, \dots, \zeta_P) = \sum_n s_n \phi_n^*(\zeta_1, \dots, \zeta_P) \quad (20)$$

Demodulating the received signal  $r(\zeta_1, \dots, \zeta_P)$  is accomplished by employing the eigenwave matched filter,  $\{\psi_n^*\}$  and the estimate  $\hat{s}_n$  is given by,

$$\hat{s}_n = \sigma_n s_n + v_n \quad (21)$$

where,  $v_n$  is the projection of noise  $v(\zeta_1, \dots, \zeta_P)$  onto the eigenwave  $\psi_n^*(\zeta_1, \dots, \zeta_P)$ .

*Proof.* Transmitting the modulated symbol  $s(\zeta_1, \dots, \zeta_P)$  over the multidimensional channel with transfer function  $H(\zeta_1, \dots, \zeta_P; \gamma_1, \dots, \gamma_Q)$ , the received signal is obtained by (22). Demodulating  $r(\zeta_1, \dots, \zeta_P)$  with  $\psi_n^*(\zeta_1, \dots, \zeta_P)$ , the estimated data  $\hat{s}_n$  is given by (23), which suggests that the demodulated symbol  $\hat{s}_n$  is the data symbol  $s_n$  multiplied a scaling factor (channel gain)  $\sigma_n$  along with AWGN, meaning there is no interference from other symbols.  $\square$

Figure 3 shows an example of 2-D eigenwave modulation using Theorem 1. At the transmitter, each data symbol,  $s_n$  is multiplied by one eigenwave  $\phi_n$ , obtained by HOGMT decomposition and then summed to create the modulated signal. The data symbols remain independent during transmission over the channel due to the joint orthogonality of eigenwaves. At the receiver, each data symbol estimate,  $\hat{s}_n$  is obtained by a matching filter using the eigenwave  $\psi_n$ , also obtained by HOGMT decomposition giving the data symbol  $s_n$  multiplied by the corresponding channel gain,  $\sigma_n$  with AWGN,  $v_n$ . Theorem 1 is applied to non-stationary channels as follows.

**Corollary 1.** (MEM modulation for non-stationary chan-

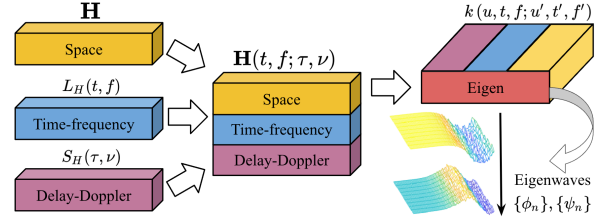


Figure 4: Eigen domain view of space, time-frequency and delay Doppler domain

nels) Given the non-stationary channel Local delay-Doppler Response (LDR),  $h_w(t, f; \tau, \nu)$  in (15) with channel kernel  $k(t, f; t', f')$ , and the input-output relation in (17), the data set  $\{s_n\}$  is modulated by MEM as

$$s(t, f) = \sum_n s_n \phi_n^*(t, f) \quad (24)$$

At the receiver, interference-free estimated symbol  $\hat{s}_n$  is obtained by demodulating the received signal  $r(t, f)$  using eigenfunctions  $\{\psi_n^*\}$  as

$$\hat{s}_n = \iint r(t, f) \psi_n^*(t, f) dt df = \sigma_n s_n + v_n \quad (25)$$

where,  $\phi_n(t, f)$  and  $\psi_n(t, f)$  are the 2-D eigenwave decomposed from  $k(t, f; t', f')$  by HOGMT.

*Proof.* It follows the same steps and deductions as in the proof of Theorem 1, except for non-stationary channels the multidimensional transfer function  $H(\zeta_1, \dots, \zeta_P; \gamma_1, \dots, \gamma_Q)$  is replaced by the channel kernel  $k(t, f; t', f')$ .  $\square$

Therefore, (25) shows that data symbols are only influenced the channel gain and AWGN, while avoiding interference in non-stationary channel by the use of MEM modulation. Furthermore, MEM modulation can also incorporate additional beamformer such as water filling, MVDR, etc., according to the desired optimization criteria [15]. However, beamformers and equalizers are out of the scope of this paper. Meanwhile, replacing  $k(t, f; t', f')$  by  $k(u, t, f; u', t', f')$  in (18), MEM modulation can directly incorporate the spatial domain without any modification. It means MEM can be directly applied to MU-MIMO channels without additional precoding.

### C. Performance analysis

**Performance in stationary channels:** Assuming the channel is ergodic, as the channel is divided into  $N$  independent subchannels (for the non-singular channel matrix/tensor,  $N$  is the multiplication of the length of each dimension), the capacity of MEM is the summation capacity of  $N$  subchannels. Then the average capacity is given by,

$$\bar{C} = \max_{\{P_n\}} \frac{1}{T} \sum_n \left(1 + \frac{P_n |\sigma_n|^2}{N_0}\right) \quad (26)$$

where,  $T$  is the time length.  $P_n$  and  $N_0$  is the power of  $s_n$  and  $v_n$ , respectively. (26) shows that, with water filling algorithm, MEM achieves the capacity for stationary channels.

$$\begin{aligned}
r(\zeta_1, \dots, \zeta_P) &= \int \dots \int H(\zeta_1, \dots, \zeta_P; \gamma_1, \dots, \gamma_Q) s(\gamma_1, \dots, \gamma_Q) d\gamma_1, \dots, d\gamma_Q + v(\zeta_1, \dots, \zeta_P) \\
&= \int \dots \int \underbrace{\left\{ \sum_{n=1}^N \sigma_n \psi_n(\zeta_1, \dots, \zeta_P) \phi_n(\gamma_1, \dots, \gamma_Q) \sum_n s_n \phi_n(\gamma_1, \dots, \gamma_Q) \right\}}_{\text{Lemma 1}} d\gamma_1, \dots, d\gamma_Q + v(\zeta_1, \dots, \zeta_P) \\
&= \int \dots \int \left\{ \sum_{n=1}^N \sigma_n s_n \psi_n(\zeta_1, \dots, \zeta_P) \underbrace{|\phi_n(\gamma_1, \dots, \gamma_Q)|^2}_{=1} + \sum_{n' \neq n}^N \sigma_n s_{n'} \psi_n(\zeta_1, \dots, \zeta_P) \underbrace{\phi_n(\gamma_1, \dots, \gamma_Q) \phi_{n'}(\gamma_1, \dots, \gamma_Q)}_{=0} \right\} d\gamma_1, \dots, d\gamma_Q + v(\zeta_1, \dots, \zeta_P) \\
&= \sum_n^N \sigma_n s_n \psi_n(\zeta_1, \dots, \zeta_P) + v(\zeta_1, \dots, \zeta_P) \tag{22}
\end{aligned}$$

$$\begin{aligned}
\hat{s}_n &= \int \dots \int r(\zeta_1, \dots, \zeta_P) \psi_n^*(\zeta_1, \dots, \zeta_P) d\zeta_1, \dots, d\zeta_P \\
&= \int \dots \int \sum_n \sigma_n s_n \psi_n(\zeta_1, \dots, \zeta_P) \psi_n^*(\zeta_1, \dots, \zeta_P) d\zeta_1, \dots, d\zeta_P + \int \dots \int v(\zeta_1, \dots, \zeta_P) \psi_n^*(\zeta_1, \dots, \zeta_P) d\zeta_1, \dots, d\zeta_P \\
&= \int \dots \int \sigma_n s_n |\psi_n(\zeta_1, \dots, \zeta_P)|^2 d\zeta_1, \dots, d\zeta_P + v_n = \sigma_n s_n + v_n \implies \text{Interference-free data symbols across all degrees of freedom} \tag{23}
\end{aligned}$$

**Performance in non-stationary channels:** The capacity for non-stationary channels is not well defined as the ergodic assumption no longer holds. In this case, we give a qualitative analysis about the optimality by using the concept of “*diversity achieving*” for the non-stationary wireless channels. We know from [1] that the total channel gain  $\mathcal{E}_H^2$  is given by,

$$\begin{aligned}
\int \dots \int |H(\zeta_1, \dots, \zeta_P; \gamma_1, \dots, \gamma_Q)|^2 d\zeta_1, \dots, d\zeta_P d\gamma_1, \dots, d\gamma_Q \\
= \sum_n^N \lambda_n \tag{27}
\end{aligned}$$

where,  $\lambda_n$  is  $n^{\text{th}}$  eigenvalue, and  $\mathbb{E}\{\sigma_n \sigma_{n'}'\} = \lambda_n \delta_{nn'}$ . Meanwhile, the power over all received symbol  $r_n$  as in (22) is,

$$\mathbb{E} \left\{ \left| \sum_n^N r_n \right|^2 \right\} = \sum_n^N \lambda_n P_n + N_0 \tag{28}$$

From (27) and (28) we find that the data symbol  $\{s_n\}$  has leveraged all the diversity gain. The reason is that the diversity of the multidimensional channel at each DoF (space, time-frequency, delay-Doppler) are merged (integral along each DoF) and then divided in the eigen domain into independently fading subchannels or eigewaves as shown in Figure 4. Therefore, eigenwaves achieve diversity in eigenspace, implying that “*diversity achieving*” for the total channel as well.

## V. RESULTS

We analyze the accuracy of MEM for non-stationary channels in Matlab using the Extended Vehicular A (EVA) model with parameters in Table II. In all simulations, we assume perfect CSI at both transmitter and receiver.

To show the effects of non-stationarity, we compared our methods with OTFS for two channels: 1) Channel-A: resolution of time evolution is one symbol. 2) Channel-B: resolution of time evolution is one subcarrier. In channel A and channel B, we generate the delay-Doppler response per symbol and per subcarrier respectively, which are also the corresponding stationarity intervals of the two channels. We also present comparisons to OTFS with time-frequency

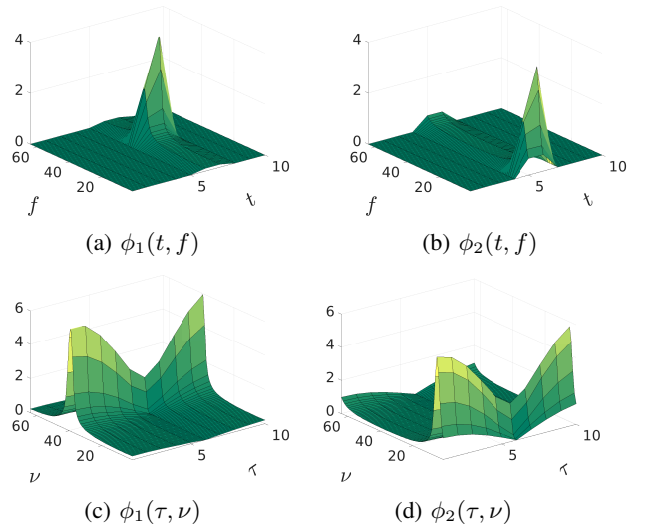


Figure 5: Eigenwaves in time-frequency,  $\phi_n(t, f)$  and delay-Doppler domain,  $\phi_n(\tau, \nu)$

single tap (TFST) [16] detector and Zero-Padded maximal ratio combining (ZP-MRC) [17] detector. For fair comparison, we also implement a Zero-Padded MEM (ZP-MEM) version, where *zero pad* is placed on eigenfunctions with least  $\sigma_n$ . ZP length is 1/8 symbol for both ZP-MEM and ZP-MRC.

To illustrate the geometry of the eigenspace, Figure 5 shows an example of *two* time-frequency eigenwaves extracted from the kernel  $k(t, f; t', f')$  by HOGMT and their representations in the delay-Doppler Domain. Unlike OFDM and OTFS, the

Table II: Parameters of Channel-A and Channel-B

Parameter	Value
Channel model	EVA model
Bandwidth	Bw = 960 KHz
Center frequency	$f_c = 5$ GHz
Subcarriers	$N_s = 64$ subcarriers
Carrier spacing	$\Delta f = 15$ KHz
Speed range	$v \in [100, 150]$ km/h
Symbols per frame	$L_F = 10$ symbols
Frame per packet	$L_P = 100$ frames
Stationarity interval	Channel A: 1 symbol; Channel B: 1 subcarrier

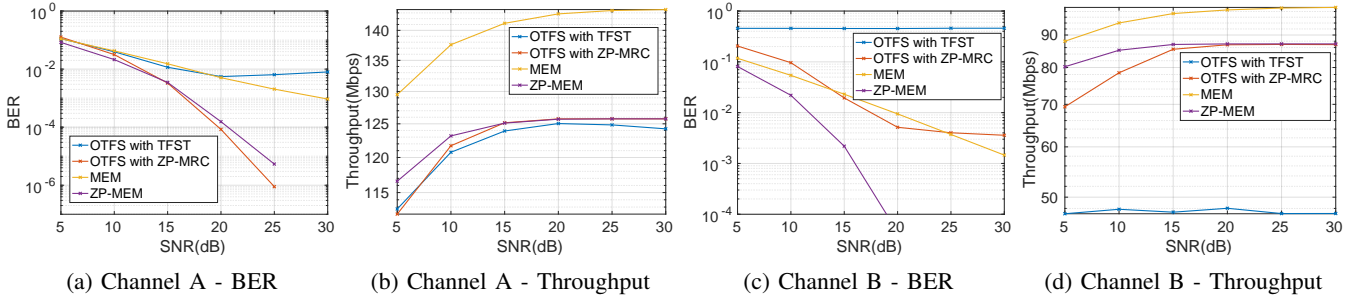


Figure 6: BER and Throughput comparison between MEM and OTFS for Channel-A and Channel-B with QPSK modulation

eigenwave is an orthonormal surface across its degrees of freedom instead of a unit division in the time-frequency or the delay-Doppler domain. However, from another perspective, consider a Hilbert space,  $\mathbb{H}_\Phi$  with basis  $\{\phi_n\}$ , then each eigenwave can be seen as a unit division in  $\mathbb{H}_\Phi$ . It means MEM analyzes the channel as one unified space (eigenspace) instead of multiple subspaces of its degrees of freedom.

Figure 6a compares the BER of MEM, ZP-MEM, OTFS with TFST and OTFS with ZP-MRC. MEM has lower BER than OTFS with TFST after 20 dB SNR, but higher BER than both ZP-MEM and OTFS with ZP-MRC. This is because demodulating data symbols on carriers (eigenwaves) with least  $\sigma_n$  will enhance the noise as well. ZP-MEM doesn't put data symbols on those eigenwaves, thereby achieving lower BER. On the other hand, ZP-MRC detector can cancel interference among OTFS symbols and thus has the similar BER with ZP-MEM. However, as shown in figure 6b, MEM has the highest throughput due to no zero pad.

Figure 6c shows the BER for Channel-B, where the stationarity interval is just one subcarrier. TFST detector doesn't work at all in this case and ZP-MRC detector has a similar BER as MEM because there are more interference at delay-Doppler domain in this channel. Both ZP-MEM and MEM are not affected because interference at delay-Doppler domain would not affect the orthogonality among eigenwaves. MEM still has the highest throughput as shown in figure 6d, while TFST performs much worse in this scenario.

We also validate the generality of MEM to higher dimension by incorporating space domain using 3GPP 38.901 UMa NLOS scenario built on QuaDriga in Matlab. The channel parameters and results are given in Appendix B [14].

## VI. CONCLUSION

In this paper, we propose a novel MEM modulation based on HOGMT decomposition. It is able to achieve orthogonality for non-stationary channels and generalizes to higher dimension by using multidimensional eigenwaves as carriers, which are jointly orthogonal across its degrees of freedom. Therefore MEM modulated symbols that are transmitted over multidimensional channel will remain independent of each other. This eliminates interference from other symbols in space, time-frequency and delay-Doppler domains without any additional precoding at the transmitter or detectors at the receiver.

## REFERENCES

- [1] Z. Zou, M. Careem, A. Dutta, and N. Thawdar, "Unified characterization and precoding for non-stationary channels," in *ICC 2022 - IEEE International Conference on Communications*, 2022, pp. 5140–5146.
- [2] D. Tse and P. Viswanath. *Fundamentals of Wireless Communications*, 2004.
- [3] R. Hadani and A. Monk, "OTFS: A New Generation of Modulation Addressing the Challenges of 5G," 2018. [Online]. Available: <https://arxiv.org/abs/1802.02623>
- [4] R. Hadani, S. Rakib, S. Kons, M. Tsatsanis, A. Monk, C. Ibars, J. Delfeld, Y. Hebron, A. J. Goldsmith, A. F. Molisch, and A. R. Calderbank, "Orthogonal time frequency space modulation," *CoRR*, vol. abs/1808.00519, 2018. [Online]. Available: <http://arxiv.org/abs/1808.00519>
- [5] P. Raviteja, K. T. Phan, Y. Hong, and E. Viterbo, "Interference Cancellation and Iterative Detection for Orthogonal Time Frequency Space Modulation," *IEEE Transactions on Wireless Communications*, vol. 17, no. 10, pp. 6501–6515, 2018.
- [6] T. Thaj, E. Viterbo, and Y. Hong, "Orthogonal time sequency multiplexing modulation: Analysis and low-complexity receiver design," *IEEE Transactions on Wireless Communications*, vol. 20, no. 12, pp. 7842–7855, 2021.
- [7] B. Cao, Z. Xiang, and P. Ren, "Low complexity transmitter precoding for mu mimo-otfs," *Digital Signal Processing*, vol. 115, p. 103083, 2021.
- [8] B. C. Pandey, S. K. Mohammed, P. Raviteja, Y. Hong, and E. Viterbo, "Low complexity precoding and detection in multi-user massive mimo otfs downlink," *IEEE transactions on vehicular technology*, vol. 70, no. 5, pp. 4389–4405, 2021.
- [9] J. Guo, C.-K. Wen, S. Jin, and G. Y. Li, "Overview of Deep Learning-based CSI Feedback in Massive MIMO Systems," 2022. [Online]. Available: <https://arxiv.org/abs/2206.14383>
- [10] F. Hlawatsch and G. Matz, *Wireless Communications Over Rapidly Time-Varying Channels*, 1st ed. USA: Academic Press, Inc., 2011.
- [11] G. Matz, "On non-wssus wireless fading channels," *IEEE Transactions on Wireless Communications*, vol. 4, no. 5, pp. 2465–2478, 2005.
- [12] P. Bello, "Characterization of Randomly Time-Variant Linear Channels," *IEEE Transactions on Communications Systems*, vol. 11, no. 4, pp. 360–393, 1963.
- [13] J. Mercer, "Functions of positive and negative type, and their connection with the theory of integral equations," *Philosophical Transactions of the Royal Society of London. Series A, Containing Papers of a Mathematical or Physical Character*, vol. 209, pp. 415–446, 1909. [Online]. Available: <http://www.jstor.org/stable/91043>
- [14] Z. Zou and A. Dutta, "Appendix for Multidimensional Eigenwave Multiplexing Modulation for Non-Stationary Channels." [Online]. Available: [https://www.dropbox.com/s/oz1p36zfa5x4fx5/ICC\\_23\\_appendix.pdf?dl=0](https://www.dropbox.com/s/oz1p36zfa5x4fx5/ICC_23_appendix.pdf?dl=0)
- [15] E. Ali, M. Ismail, R. Nordin, and N. F. Abdulah, "Beamforming techniques for massive mimo systems in 5g: overview, classification, and trends for future research," *Frontiers of Information Technology & Electronic Engineering*, vol. 18, no. 6, pp. 753–772, 2017.
- [16] Y. Hong, T. Thaj, and E. Viterbo, *Delay-Doppler Communications: Principles and Applications*, 1st ed. USA: Elsevier Science., 2022.
- [17] T. Thaj and E. Viterbo, "Low complexity iterative rake decision feedback equalizer for zero-padded OTFS systems," *IEEE transactions on vehicular technology*, vol. 69, no. 12, pp. 15 606–15 622, 2020.